

Microstructure, phase transformation and wear behavior of Cu–10%Al–4%Fe alloy processed by ECAE

L.L. Gao^{a,*}, X.H. Cheng^{a,b}

^a School of Mechanical Engineering, Shanghai Jiao Tong University, Shanghai 200030, PR China

^b National Power Traction Laboratory of Southwest Jiaotong University, Chengdu 610031, PR China

Received 26 January 2007; received in revised form 20 March 2007; accepted 21 March 2007

Abstract

The aim of this study is to determine optimum processing conditions of equal channel angular extrusion (ECAE) for a two-phase alloy and to investigate the effect of ECAE on microstructure, phase transformation and tribological properties of the alloy. A commercial aluminum bronze alloy (Cu–10%Al–4%Fe) produced by hot-rolling was subjected to ECAE process at 550, 600 and 650 °C, respectively. Experimental results showed that the extrusion temperature must be higher than the eutectoid reaction temperature of the alloy. Optical microscope was used to study the microstructure of the alloy. The grains of the alloy were refined after ECAE and gradually reduced with the increase of pass number of ECAE. The mechanical and tribological properties of the alloy were significantly improved after ECAE. In addition, phase transformation temperature of the alloy decreased after ECAE process.

© 2007 Elsevier B.V. All rights reserved.

Keywords: Equal channel angular extrusion; Microstructure; Phase transformation; Wear

1. Introduction

Equal channel angular extrusion technique is a severe plastic deformation process which can produce bulk ultra fine-grained materials by simple shear [1]. One important advantage of ECAE is that it imposes much higher plastic strain during pressing without reducing the cross-sectional area of working billets, resulting in unique combinations of mechanical properties and grain size. Active research efforts have been made recently, and successful applications have been reported for various materials such as pure copper [2–4], Al alloys [5–8], magnesium alloys [9,10], Ti alloys [11,12], etc.

The effect of ECAE on microstructure and mechanical properties of pure copper has been investigated in detail. However, previous ECAE studies are mostly concerned with producing an ultra fine-grained microstructure from single-phase alloys. For single-phase alloys with high ductility, ECAE is usually carried out at room temperature. For two-phase alloy, an increase of the extrusion temperature is generally required to increase its ductility because the two-phase microstructure with a high volume

fraction of the second phase is too brittle to be deformed during ECAE at low temperature [13]. Considering the industrial importance of two-phase materials, it is essential to establish optimum processing conditions of such difficult-to-fabricate materials to study the effects of ECAE on microstructural changes and mechanical properties of two-phase alloys.

In this study, a commercial aluminum bronze alloy (Cu–10%Al–4%Fe) was chosen to determine its suitable processing temperature for ECAE, and the effect of ECAE on the microstructure, phase transformation behavior and wear properties of the alloy was also investigated.

2. Experimental procedure

A commercial aluminum bronze alloy, Cu–10%Al–4%Fe (the concentration of alloying elements was given in wt.%) was used as experimental material for ECAE. The billets 9.6 mm × 9.6 mm in cross-section and 100 mm long were cut from a rod obtained in the as-rolling condition. The die used for ECAE consisted of two rectangular channels of cross-section area 10 mm × 10 mm intersecting at angle of 90°. The billets and dies were heated in a furnace at temperature of 550, 600 and 650 °C for 30 min. The actual temperatures of billets during ECAE were tested by a thermocouple thermometer.

* Corresponding author. Tel.: +86 21 62932404; fax: +86 21 34205880.
E-mail address: gaoleilei@sjtu.edu.cn (L.L. Gao).

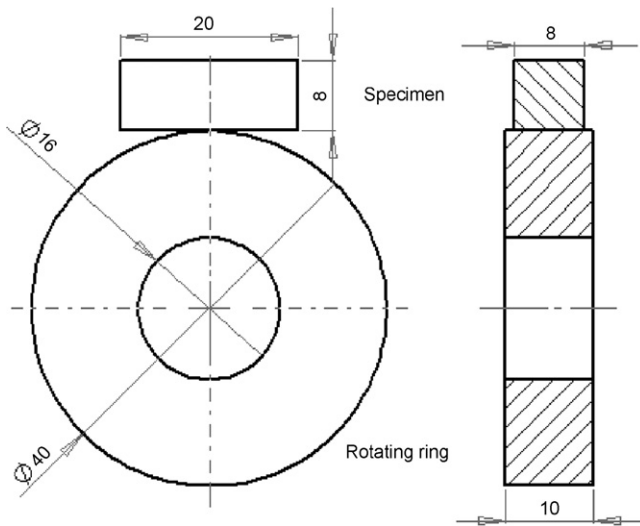


Fig. 1. Contact schematic diagram for the frictional pair (unit: mm).

Optical microscope was used to study the microstructure of the alloy. The specimens for microstructure observation were cut along the extrusion direction. Vickers microhardness measurements were taken with a load of 50 g applied for 13 s. The specimens for tensile test were machined from the as-received and the extruded billets with gauge length of 25 mm and cross-section of 2 mm × 2 mm. The tensile test was conducted at room temperature with a strain rate of 10^{-3} s^{-1} . Differential scanning calorimeter (DSC) measurement was carried out to analyze the changes of phase transformation behavior of the alloy before and after ECAE.

The friction and wear behavior of the aluminum bronze alloy blocks sliding against a GCr15 steel ring was evaluated on an M-2000 model ring-on-block test rig. The contact schematic diagram of the frictional pair is shown in Fig. 1. The blocks in a size of 20 mm × 8 mm × 8 mm were made of the alloy, and the rings of $\varnothing 40 \text{ mm} \times 10 \text{ mm}$ were made of GCr15 steel. The chemical compositions of the GCr15 steel are given in Table 1.

The tests were carried out at a linear velocity of 0.42 m/s, sliding distance of 2500 m, ambient temperature around 20 °C and relative humidity 50%. During the tests, the load was increased gradually until the maximum possible load could be applied or until seizure took place. The friction coefficient, μ , is calculated by the expression:

$$\mu = \frac{T}{F_N R} \quad (1)$$

where T is the friction torque recorded by the tester (N m), F_N the normal force (N) and R is the radius of the ring (m).

Table 1
Chemical composition of the GCr15 steel (wt.%)

C	0.75–0.85
Mn	0.20–0.40
P	≤0.027
S	≤0.020
Si	0.15–0.35
Cr	1.30–1.65

A characteristic value, which describes the wear performance under the chosen conditions for a tribosystem, is the specific wear rate:

$$K = \frac{\Delta V}{F_N L} \quad (2)$$

$$\Delta V = \left[R^2 \arcsin \frac{b}{2R} - \frac{b \sqrt{R^2 - (b/2)^2}}{2} \right] B \quad (3)$$

where L is the sliding distance (m), ΔV the worn volume loss (m^3), b the width of the wear track (m) and B is the width of specimen (m).

The morphologies of worn surfaces were examined by using a scanning electron microscope (SEM, Model: S-520, Hitachi Inc.).

3. Results and discussion

3.1. Effect of extrusion temperature

Fig. 2 shows the external appearances of the billets with ECAE after one pass at three different temperatures. It can be seen from Fig. 2 that, at heating temperature of 550 and 600 °C, the ECAE process is not carried out successfully. At heating temperature of 550 °C, the billet breaks catastrophically when passing through the die. At heating temperature of 600 °C, there are some extensive cracks on the surface of the billet, although the billet does not break. When using a higher heating temperature of 650 °C, the ECAE process is carried out successfully without breaking and without any surface cracks of the billet. In addition, the extruded material with ECAE after one pass is pressed easily at heating temperature of 650 °C through six passes without surface cracks.

It can be seen from Fig. 3 that microstructure of the as-received aluminium bronze alloy consists of two phases, α phase and ($\alpha + \gamma_2$) eutectoid structure. The γ_2 phase is brittle and difficult to deform during ECAE. The eutectoid reaction temperature is 565 °C according to copper–aluminum diagram. Above this temperature, eutectoid reaction ($\alpha + \gamma_2 \rightarrow \beta$) occurs and γ_2 phase vanishes. At heating temperature of 550 °C, ECAE is carried out below the eutectoid reaction temperature and γ_2 phase still exists in the microstructure of the alloy. ECAE process fails because of the brittle nature of γ_2 phase. At heating temperature of 600 °C, the temperature of billet and die drops when the billet and die are taken from furnace and the actual temperature of the billets during ECAE process is 560 °C. Thus, extensive cracks occur on the surface of the specimen because of heat losses. With the heating temperature increases, for example 650 °C (the actual temperature of is 605 °C), ECAE process can be performed successfully. It is reasonably explained that the temperature of the billet is higher than the eutectoid reaction temperature after heat losses and γ_2 phase is replaced by β phase with high ductility.



Fig. 2. Appearances of the aluminum bronze billets subjected to ECAE at (a) 550 °C, (b) 600 °C and (c) 650 °C.

3.2. Effect of ECAE on microstructure and mechanical properties

Fig. 3 shows the optical images of the specimens without ECAE and with ECAE after three and six passes. It is apparent

that α phase and the second phase are elongated along rolling direction (vertical direction) and α phase parallels the second phase with few intersections before ECAE, as shown in Fig. 3(a). After three passes of ECAE, the microstructure mainly consists of parallel boundaries as shown in Fig. 3(b). Most of the grain

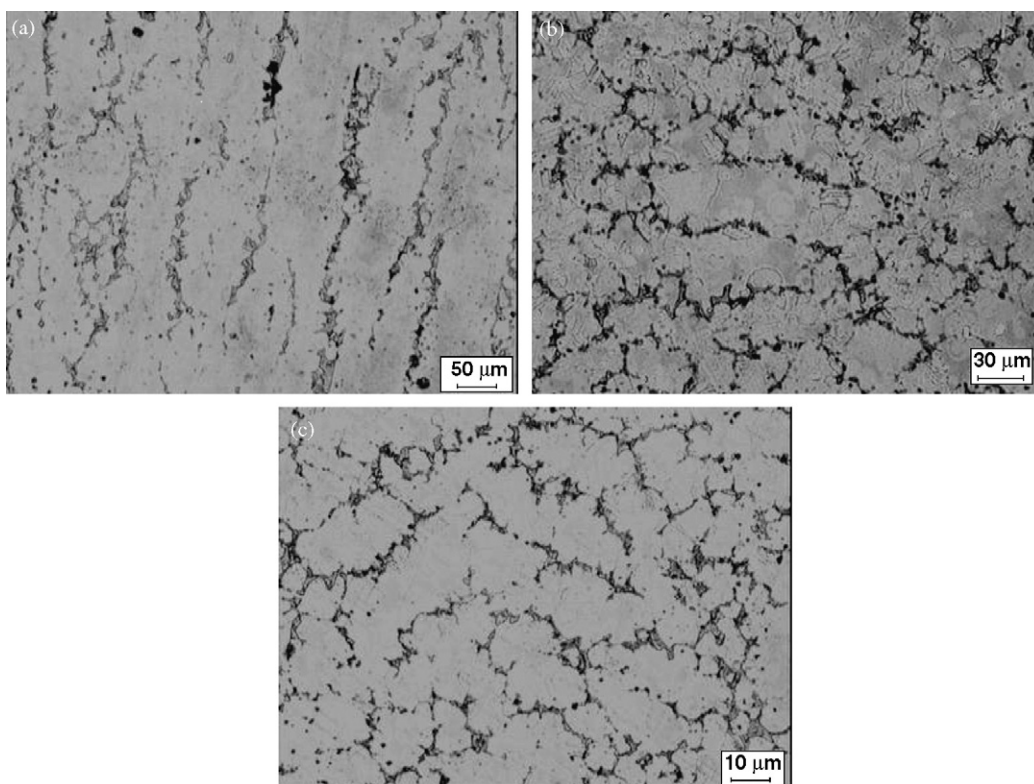


Fig. 3. Microstructure of aluminum bronze specimens: (a) without ECAE, (b) after ECAE with three passes and (c) after ECAE with six passes.

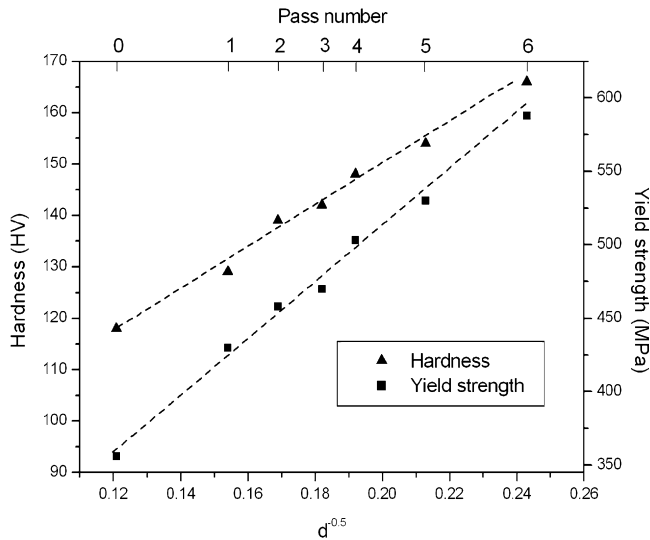


Fig. 4. Effect of ECAE on grain size and mechanical properties of aluminum bronze specimens.

boundaries still align along the extrusion direction (horizontal direction), but some boundaries deviate from the extrusion direction. Therefore, it can be seen that in some areas, some equiaxed grains occur and α phase intersects the second phase. The grain boundaries are no longer straight, but more curved than the boundaries without ECAE. After six passes of ECAE, the grain size is refined remarkably and the distribution of the second phase particles is more homogeneous, as shown in Fig. 3(c).

The effect of ECAE on grain size and mechanical properties of the alloy is shown in Fig. 4. It can be seen that the hardness and yield strength of specimens after ECAE is higher than that of specimen without ECAE. The mechanical properties increase and grain size decreases with the increase of pass number.

Grain refinement is commonly known to increase the hardness and the strength of grained materials. It is well recognized that the yield stress $\sigma_{0.2}$ and the hardness HV of a metallic material increase with decreasing grain size d . In particular, the Hall–Petch equation expresses the grain size dependence of strength and hardness. In terms of strength and hardness, the Hall–Petch equations are

$$\sigma_{0.2} = \sigma_0 + kd^{-0.5} \quad (4)$$

$$H = H_0 + k'd^{-0.5} \quad (5)$$

where σ_0 and H_0 are constants relating to the material of infinite grain size; k and k' are constants, and d is the diameter of grain. The Hall–Petch effect in grain refinement materials is attributed to the grain boundaries acting as efficient obstacles to dislocations. Consequently, a dislocation pile-up can be formed against a grain boundary inside a grain. From Fig. 4 it can be seen that the hardness and yield strength follow almost a linear trend with the $(d)^{-0.5}$. Hence it is analogous to the Hall–Petch relation.

3.3. Effect of ECAE on phase transformation behavior

Fig. 5 shows DSC curves of the specimens without ECAE and after one pass of ECAE. For each specimen, a broad endothermic

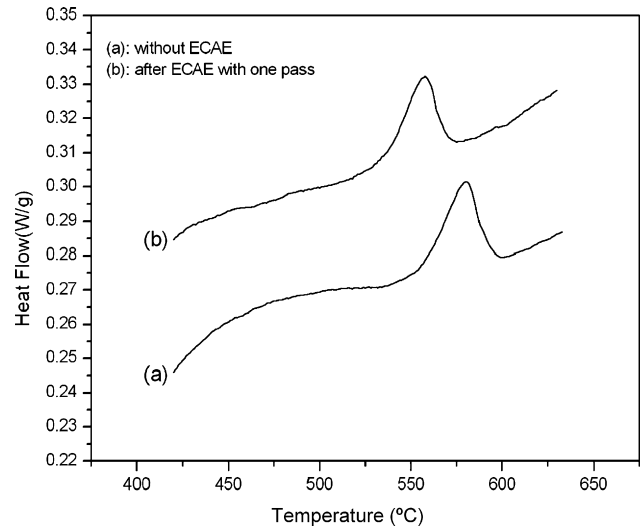


Fig. 5. DSC curves of aluminum bronze specimens: (a) without ECAE and (b) after ECAE with one pass.

mic peak is observed on the DSC curve corresponding to the eutectoid reaction. For the specimen without ECAE, the onset of the endothermic peak is about 542 °C and its maximum is around 561 °C, as shown in Fig. 5(a). After one pass of ECAE, the maximum of the endothermic peak decreases to 545 °C, as shown in Fig. 5(b). Variation of the maximum temperature of the endothermic peak versus pass number is shown in Fig. 6. It can be seen that with the increase of the pass number of ECAE, the maximum temperature of the endothermic peak decreases and it reaches the lowest after six passes. The result suggests that ECAE process can significantly decrease the eutectoid reaction temperature of the alloy.

From Fig. 3, it is distinctly seen that $(\alpha + \gamma_2)$ eutectoid structure nucleates at α phase boundaries. After ECAE, the grains of the specimens are refined and a large number of nucleation sites are available when the eutectoid structure nucleates at the grain boundaries [14]. In addition, many dislocations are introduced

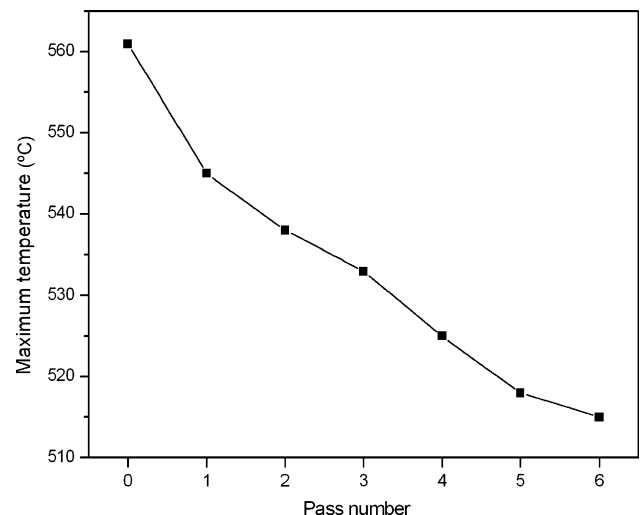


Fig. 6. The maximum temperature of endothermic peak on DSC curves as a function of pass number.

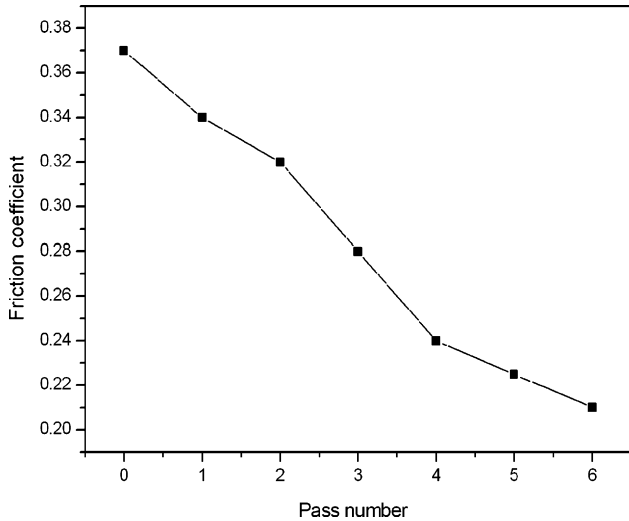


Fig. 7. Friction coefficient of specimens vs. pass number at 100 N normal load and sliding speeds of 0.42 m/s.

during ECAE, which increases the driving force for nucleation of the eutectoid reaction [15]. Thus, nucleation is achieved at lower temperatures and the eutectoid reaction temperature of the alloy decreases markedly after ECAE.

3.4. Effect of ECAE on wear properties

Fig. 7 shows the friction coefficients of the specimens with different pass number under the load of 100 N and the sliding speeds of 0.42 m/s. It is noticeable that the effect of ECAE on friction coefficient is evident, the friction coefficient decreases considerably with increasing pass number and the specimen with ECAE after six passes has the lowest levels in friction coefficient.

The variations in wear rate with load for specimens with and without ECAE are shown in Fig. 8. It can be seen that the wear rate of all specimens increases with the increase of the load. Under the loads from 20 to 260 N, specimen with six passes of ECAE shows the lowest wear rate, while specimen without ECAE presents the highest. The wear rate decreases with

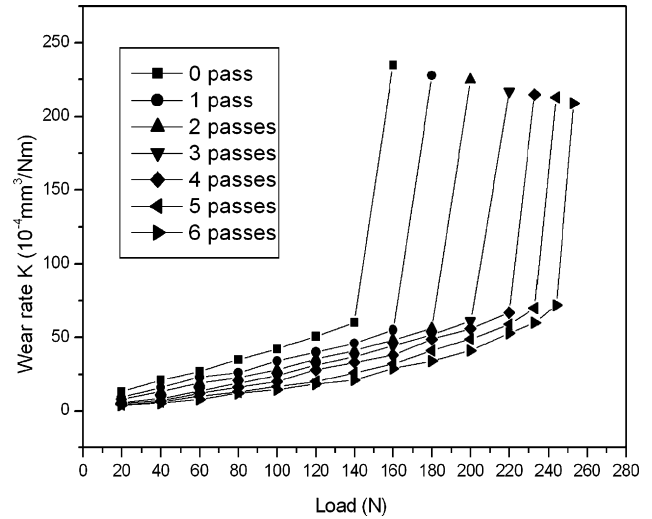


Fig. 8. Variations of wear rate with load for the aluminum bronze specimens with different pass number.

the increase of pass number, which indicates that the wear rate decreases with the decrease of grain size. It is also can be seen that the wear resistance of untreated specimen is poor compared with that of ECAE-treated specimens. The resistance to seizure of the alloy increases after ECAE. The seizure load for specimens increases from 160 N before ECAE to 253 N after ECAE with six passes. The wear rate of all the specimens increases gradually with the increase of load before seizure occurs while it shows a dramatically increase as the load reaches the seizure value. This is due to the test specimens becoming welded to the disc at high loads and extensive wear occurs during wear, as shown in Fig. 9.

The reason for the superior wear performance of the ECAE-treated specimens is due to the grain refinement of the alloy after ECAE. It is well known that shear strength depends on the hardness of the material [16]. Thus, the reason for the decrease of the wear rate and the drop of the friction coefficient can be due to the increase of the hardness of the alloy. The improvement of wear resistance with the increase of hardness, in this study due

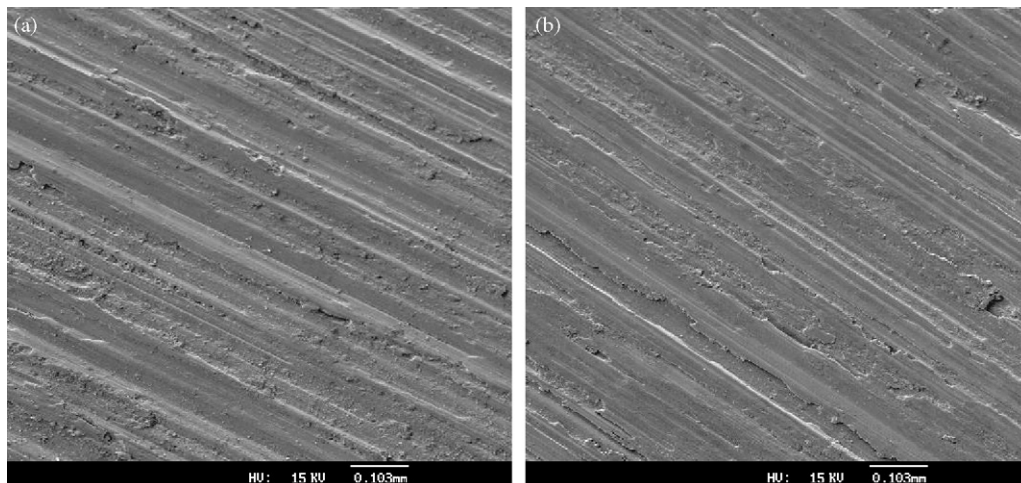


Fig. 9. SEM morphologies of the worn surface of aluminum bronze under seized load: (a) without ECAE and (b) after ECAE with six passes.

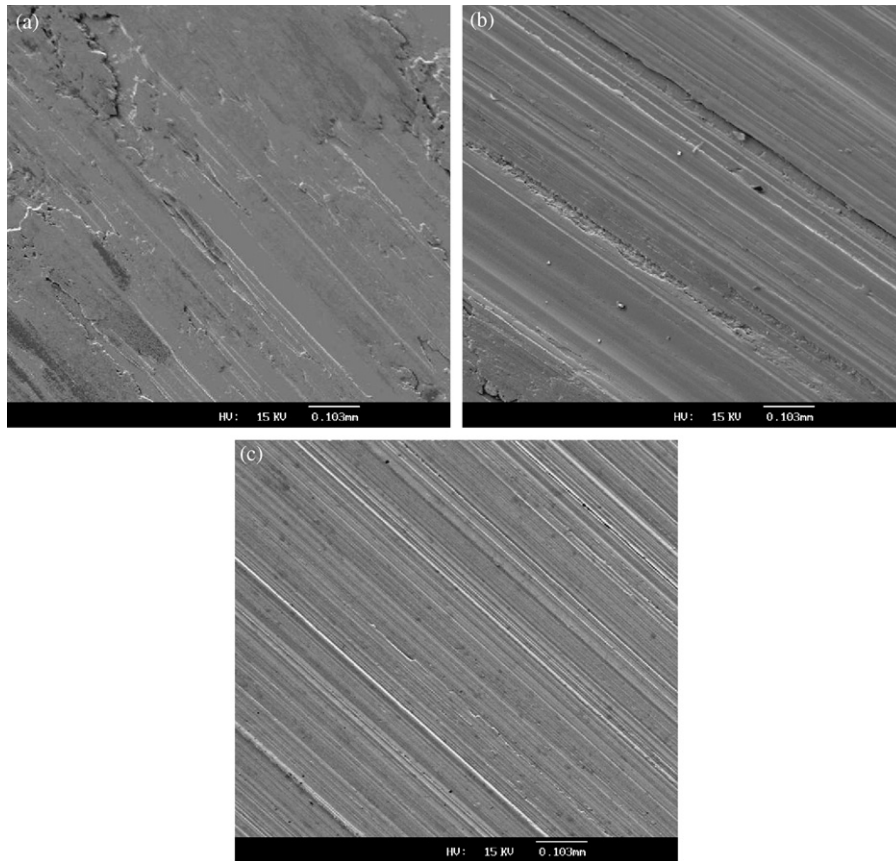


Fig. 10. SEM morphologies of the worn surface of aluminum bronze specimens with 100 N load: (a) without ECAE, (b) after ECAE with three passes and (c) after ECAE with six passes.

to the grain size reduction, can be expressed using Archard's law. Traditional Archard's law can be expressed as follows:

$$Q = K \frac{LN}{H} \quad (6)$$

where Q is the volumetric wear loss, N the applied load, L the total sliding distance, K the wear coefficient and H is the hardness of the wear surface. For the specimens after ECAE with different pass number, the hardness increases, as shown in Fig. 4. As a result, the wear resistance of the alloy improves remarkably after ECAE.

Moreover, the improvement in wear resistance and the decrease of friction coefficient as a result of grain size reduction can be further confirmed by the worn surface morphology of specimens with different pass number as shown in Fig. 10. For the specimen without ECAE, the wear track shows the larger extent of adhesion wear and severe plastic deformation in the sliding direction, which results in the larger extent of delaminating, as shown in Fig. 10(a). Such a wear mechanism is due to the lower hardness of the specimen without ECAE. It is reasonable to conclude that there is a larger tendency for plastic deformation and severe adhesion; this in turn increased the probability of formation of asperity junctions resulting in a much higher friction coefficient. When the grain size of specimens decrease with the pass number increase, as can be seen in Fig. 10(b), the plastic deformation and adhesion wear decreased a lot, which

results in the decrease of wear rate. The decrease of grain size can increase its hardness, thereby reduces the adhesive wear of the alloy. As a result, the observed plastic deformation of surfaces of specimens with ECAE becomes less intensive as the grain size decreases. And after six passes of ECAE, the features of delamination and adhesion wear of specimens are replaced by abrasive wear as shown in Fig. 10(c). Consequently, the specimens with ECAE show a decrease both in the friction coefficient and wear rate with the increase of hardness as a result of grain size decrease.

4. Conclusions

- It is demonstrated that ECAE for aluminum bronze alloy can only be carried out at a temperature that is above the eutectoid reaction temperature of the alloy. After ECAE, the alloy has more homogeneous fine-grained structure than the as-received one and the grain size of the alloy progressively decreases with the increase of the pass number of ECAE.
- The improvement in the mechanical properties of the alloy is due to grain refinement. ECAE can decrease the eutectoid reaction temperature of the alloy and affect phase transformation behavior of the alloy.
- The wear properties of the alloy are improved after ECAE. This is because the decrease of grain size can increase its hardness, thereby reduces the adhesive wear of the alloy.

Acknowledgements

This research is financially supported by National Natural Science Foundation of China (Grant No. 50275093), the open fund of State Key Laboratory of Tribology, Tsinghua University and Instrumental Analysis Center of Shanghai Jiao Tong University.

References

- [1] W.H. Huang, C.Y. Yu, P.W. Kao, C.P. Chang, *Mater. Sci. Eng. A* 366 (2004) 221.
- [2] M. Haouaoui, K. Ted, E.A. Payzant, *Acta Mater.* 53 (2005) 801.
- [3] S.D. Wu, Z.G. Wang, C.B. Jiang, G.Y. Li, I.V. Alexandrov, R.Z. Valiev, *Mater. Sci. Eng. A* 387 (2004) 560.
- [4] W.H. Huang, L. Chang, P.W. Kao, C.P. Chang, *Mater. Sci. Eng. A* 307 (2001) 113.
- [5] U. Chakkingal, P.F. Thomson, *J. Mater. Process. Technol.* 117 (2001) 169.
- [6] J.R. Bowen, O.V. Mishin, P.B. Prangnell, *Scripta Mater.* 47 (2002) 289.
- [7] Y.C. Chen, Y.Y. Huang, C.P. Chang, P.W. Kao, *Acta Mater.* 51 (2003) 2005.
- [8] W.Q. Cao, A. Godfrey, Q. Liu, *Mater. Sci. Eng. A* 361 (2003) 9.
- [9] S.R. Agnew, J.A. Horton, T.M. Lillo, D.W. Brown, *Scripta Mater.* 50 (2004) 377.
- [10] T. Liu, W. Zhang, S.D. Wu, C.B. Jiang, S.X. Li, Y.B. Xu, *Mater. Sci. Eng. A* 360 (2003) 345.
- [11] Z. Li, G. Xiang, X. Cheng, *Mater. Des.* 27 (2006) 324.
- [12] Z. Li, X. Cheng, Q. ShangGuan, *Mater. Lett.* 59 (2005) 705.
- [13] Z.C. Wang, P.B. Prangnell, *Mater. Sci. Eng. A* 328 (2002) 87.
- [14] M. Murayama, Z. Horita, K. Hono, *Acta Mater.* 49 (2001) 21.
- [15] N. Saito, M. Mabuchi, M. Nakanishi, I. Shigematsu, G. Yamauchi, M. Nakamura, *J. Mater. Sci.* 36 (2001) 3229.
- [16] A.K. Prasada Rao, K. Das, B.S. Murty, M. Chakraborty, *Wear* 261 (2006) 133.